

Tactile Display Using Elastic Waves

Takaaki NARA, Taro MAEDA, Yasuyuki YANAGIDA and Susumu TACHI

Faculty of Engineering
University of Tokyo
Bunkyo-ku, Tokyo
nara@star.t.u-tokyo.ac.jp

Abstract

As a basis for tactile display, it is important to understand the mechanism of tactile sensation. So, we analyze elastic waves inside a finger in tactile exploration with a two-layered, half-infinite elastic finger model, and derive a mapping from shapes of objects to displacements of mechanoreceptors. It is shown that the mapping from displacements of the finger surface to displacements of mechanoreceptors is a one-to-one mapping. Therefore, it is necessary to create the same displacements of the finger surface as in actual exploration for tactile virtual reality(VR). However, the mapping from shapes of objects to displacements of the finger surface is shown to be a many-to-one mapping because of the mechanical property of skin. So, we use the envelope of the amplitude-modulated Lamb wave on an elastic plate as an alternative shape to the real object, because its shape is easily controlled. The generation of the wave is confirmed with an experimental device of silicon rubber vibrated by voice coils.

1 Introduction

The purpose of this study is the development of a tactile display, which provides the feel of roughness, ruggedness, or small surface textures of objects in tactile exploration. Many tactile displays using variable actuators have been proposed [1]-[4]. However, physical phenomena of tactile sensation have not been adequately analyzed, therefore it is difficult to predict physical states inside the finger, and tactile sensation as a result, which are evoked by some stimulus generated by the display. The study of the mechanism of tactile sensation is important because it delineates what should be displayed for tactile VR.

Static skin deformations are analyzed in detail with the elastic finger model.[5] [6] However, dynamic phenomena should also be investigated because tactile sensation is obtained by active exploration. Indeed, a tactile exploration gives a spatio-temporal displacement, or stress distribution on a finger surface, which

generates elastic waves inside the finger. Mechanoreceptors embedded in the upper layer of the finger detect the quantity of the wave, and as a result, they are activated and transmit signals to the brain. This is a sketch of how tactile sensation occurs, thus elastic waves in the finger are essential for tactile sensation. In this paper we analyze the elastic waves inside the finger using a two-layered, elastic half space model of the finger.

Now, let us consider that tactile sensation is obtained because a physical state of the outside world is 'mapped' on a physical state of the mechanoreceptors. Concretely, the state of the outside world is a geometric shape of an object, and the state of mechanoreceptors is a set of their displacements. Then, the expression of the mapping from the shapes of the objects to the displacements of the mechanoreceptors can be derived by the analysis with the elastic finger model.

Here, it is a problem for VR whether the mapping is one-to-one or many-to-one, because a many-to-one mapping can produce the same sensation from two different shapes of the objects. (Fig.1) Although generating an arbitrary shape instantly is very difficult, the possibility exists that the real sensation is evoked by the substitute shape which is created more easily than the real shape, if the mapping is many-to-one.

A brief overview of this paper is as follows. First, in the analysis with the two-layered elastic half space model, the mapping F from the displacements of the skin surface to displacements of mechanoreceptor is derived. It is shown that F is one-to-one because of the characteristic structure of the finger in section 2. Second, the mapping C from shapes of objects to the displacements of the skin surface is considered, and shown to be many-to-one because of the mechanical response character of the skin (section 3). Then, we suggest a tactile display using the many-to-one property of the mapping. The essence of the method is that deformation of the finger surface in touching the amplitude-modulated elastic wave is the envelope of

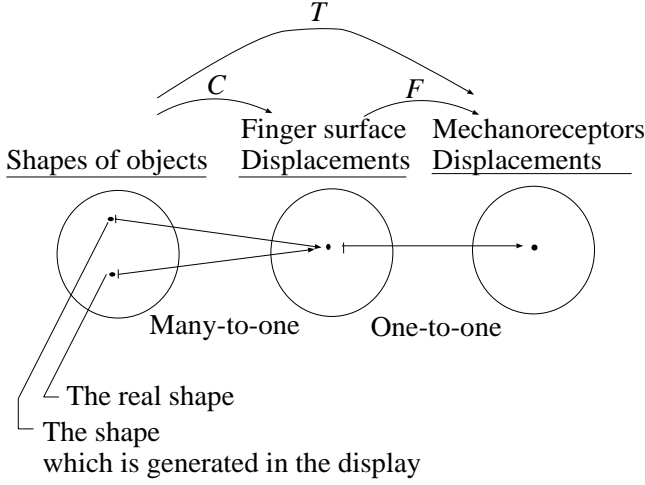


Figure 1: **VR by Many-to-one mapping.** C is determined by contact between the object and the skin. F is determined by the elastic media in the finger. T , which is a composite mapping of C and F , represents the total tactile operation.

the wave. Because a wave length and a travelling velocity of the envelope are controllable, the arbitrary displacement of the finger surface, and the arbitrary displacements of the mechanoreceptors as a result, can be formed. The experimental device with which the basic phenomena of the above principle can be confirmed is described in section 4.

2 Analysis of tactile sensation

2.1 Two-layered elastic half-space model of the finger

Mechanics of tactile sensation have been analyzed with models of an elastic media of a finger to predict the neural responses evoked by the stimuli applied to a skin surface. [5] used a homogeneous, isotropic, incompressible, linearly elastic half-space model of a finger. This simple and idealized model predicted SAI response profiles well, but it treated only static stimuli. [6] also analyzed static problems with more detailed models composed of linear elastic media of variable shapes by finite element calculations.

Dynamic mechanical properties of the skin has been studied primarily for medical motives.[7]-[11] However, the most detailed analysis with a layered elastic model of the finger in [11] has focused only on SH waves which vibrate parallel to the skin surface. The more general analysis dealing with deformations parallel and perpendicular to the skin is required for the phenomenon of tactile sensation.

So, in this paper, a two-dimensional problem is discussed with the two-layered, elastic half-space finger model shown in Fig.2. We set x -axis parallel to the skin surface, and z -axis perpendicular to the skin surface. The plane, $z = 0$, is the boundary between the first(upper) and the second(lower) layers. The first layer represents epidermis and dermis with a depth of H , and lays in the region $0 < z < H$. The second layer represents the subcutaneous tissue and lays in the region $z < 0$. Both layers are assumed to be homogeneous, isotropic, linearly elastic media, and have different elastic constants respectively.

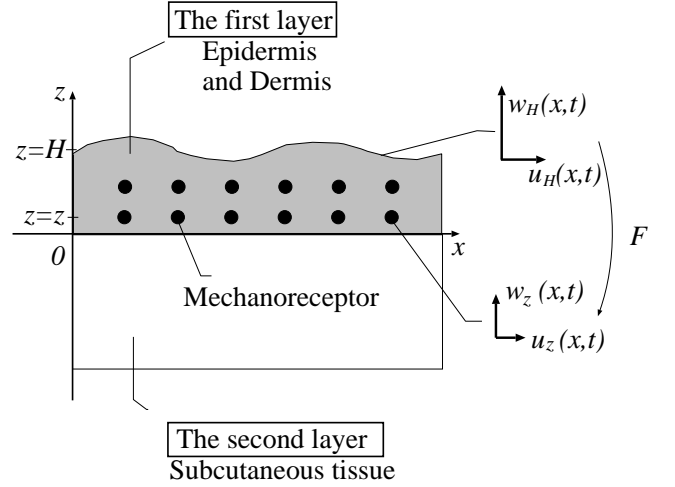


Figure 2: **Two-layered half-infinite elastic model of the finger.**

When tactile exploration is conducted, two-directional (x -directional and z -directional) displacements, or stresses, are given on the finger surface as a boundary condition. Because stresses and displacements at $z = H$ can be transformed to each other, we take boundary conditions of displacements here.

The following notation is used:

- (u_i, w_i) : Displacement in the i -th layer ($i = 1, 2$)
- $(u_H, w_H) = (u_1, w_1)|_{z=H}$
- $(u_z, w_z) = (u_1, w_1)|_{z=z}$
- λ_i, μ_i : Lamé's Constants
- μ_i : Rigidity
- ρ_i : Density
- α_i : P-wave velocity
- β_i : S-wave velocity

The problems dealt with in section 2 are as follows:

First, a derivation of the mapping F from (u_H, w_H) to (u_z, w_z) . In other words, we express the displacements of the mechanoreceptors in terms of the displacements of the skin surface. The result is (26) in section 2.2. By using this result, an amplitude distribution inside the finger during the exploration of a sinusoidal shape is shown in section 2.3.

Second, a discussion of whether F is one-to-one or many-to-one. (section 2.4) The result is one-to-one because of the characteristic structure of the finger—the upper layer being stiffer than the lower layer; $\mu_1 > \mu_2$.

2.2 Derivation of the mapping F

2.2.1 Basic equations

Displacement potentials in the i -th layer: (ϕ_i, ψ_i) , which have a relation with (u_i, w_i) as

$$u_i = \frac{\partial \phi_i}{\partial x} - \frac{\partial \psi_i}{\partial z}, \quad w_i = \frac{\partial \phi_i}{\partial z} + \frac{\partial \psi_i}{\partial x}, \quad (1)$$

satisfy the wave equations

$$\frac{1}{\alpha_i^2} \frac{\partial^2 \phi_i}{\partial t^2} = \nabla^2 \phi_i, \quad \frac{1}{\beta_i^2} \frac{\partial^2 \psi_i}{\partial t^2} = \nabla^2 \psi_i. \quad (2)$$

The solution of (2) is assumed as follows:[12] (Here, $e^{j(kx+\omega t)}$ is excluded.)

$$\begin{aligned} \phi_1 &= (P \cosh r_1 z + Q \sinh r_1 z) & \phi_2 &= P' e^{r_2 z} & (3) \\ \psi_1 &= (A \cosh s_1 z + B \sinh s_1 z) & \psi_2 &= A' e^{s_2 z} & (4) \\ r_i &= \sqrt{k^2 - k_{\alpha_i}^2} & s_i &= \sqrt{k^2 - k_{\beta_i}^2} & k_{\alpha_i} = \frac{\omega}{\alpha_i} \quad k_{\beta_i} = \frac{\omega}{\beta_i} & (5) \end{aligned}$$

If unknown coefficients P, Q, A, B, P', A' in (3),(4) can be expressed by (u_H, w_H) , we substitute them into (3),(4) and (1), so that we obtain the expression (u_z, w_z) in terms of (u_H, w_H) .

2.2.2 Boundary conditons

The solution assumed in (3),(4) should be subject to the following six boundary conditions.

First, the continuity conditions of stress and displacement at $z = 0$.

$$\bullet \quad (T_{zz})_1 = (T_{zz})_2 \quad \text{at } z = 0 \quad (6)$$

$$\bullet \quad (T_{zx})_1 = (T_{zx})_2 \quad \text{at } z = 0 \quad (7)$$

$$\bullet \quad u_1 = u_2 \quad \text{at } z = 0 \quad (8)$$

$$\bullet \quad w_1 = w_2 \quad \text{at } z = 0 \quad (9)$$

Next, the displacement boundary conditions at $z = H$ in tactile exploration.

$$\bullet \quad (u_1)_{z=H} = u_H = u_H^* e^{j(kx+\omega t)} \quad \text{at } z = H \quad (10)$$

$$\bullet \quad (w_1)_{z=H} = w_H = w_H^* e^{j(kx+\omega t)} \quad \text{at } z = H \quad (11)$$

(6) and (8) reduce to the expression of P, B in terms of P', A' as

$$\begin{pmatrix} P \\ B \end{pmatrix} = \frac{k^2}{k_{\beta_1}^2} \begin{pmatrix} X & \frac{s_2}{k} W \\ \frac{k}{s_1} Z & \frac{s_2}{s_1} Y \end{pmatrix} \begin{pmatrix} P' \\ A' \end{pmatrix}. \quad (12)$$

In the same way, Q, A are expressed by P', A' from (7), (9), as

$$\begin{pmatrix} Q \\ A \end{pmatrix} = \frac{k^2}{k_{\beta_1}^2} \begin{pmatrix} \frac{r_2}{r_1} Y & \frac{k}{r_1} Z \\ \frac{r_2}{k} W & X \end{pmatrix} \begin{pmatrix} P' \\ A' \end{pmatrix}, \quad (13)$$

where μ, X, Y, Z, W are defined as

$$\mu = \frac{\mu_2}{\mu_1}, \quad (14)$$

$$X = \mu \frac{k_{\beta_2}^2}{k^2} - 2(\mu - 1), \quad (15)$$

$$W = 2(\mu - 1), \quad (16)$$

$$Z = \mu \frac{k_{\beta_2}^2}{k^2} - \frac{k_{\beta_1}^2}{k^2} - 2(\mu - 1), \quad (17)$$

$$Y = \frac{k_{\beta_1}^2}{k^2} + 2(\mu - 1). \quad (18)$$

On the other hand, (10), (11) are reduced to

$$\begin{aligned} & \begin{pmatrix} -k \cosh r_1 H & s_1 \cosh s_1 H \\ r_1 \sinh r_1 H & -k \sinh s_1 H \end{pmatrix} \begin{pmatrix} P \\ B \end{pmatrix} \\ & + \begin{pmatrix} -k \sinh r_1 H & s_1 \sinh s_1 H \\ r_1 \cosh r_1 H & -k \cosh s_1 H \end{pmatrix} \begin{pmatrix} Q \\ A \end{pmatrix} \\ & = \begin{pmatrix} u_H^* \\ w_H^* \end{pmatrix}, \end{aligned} \quad (19)$$

by using (1),(3),(4). Substituting (12) and (13) into (19), we obtain

$$G_z|_{z=H} \cdot \begin{pmatrix} P' \\ A' \end{pmatrix} = \frac{k_{\beta_1}^2}{k^3} \begin{pmatrix} u_H^* \\ w_H^* \end{pmatrix}, \quad (20)$$

where

$$G_z = \begin{pmatrix} g_1 & g_2 \\ g_3 & g_4 \end{pmatrix}, \quad (21)$$

$$\begin{aligned}
g_1 &= -X \cosh r_1 z + Z \cosh s_1 z \\
&\quad - \frac{r_2}{r_1} Y \sinh r_1 z + \frac{s_1 r_2}{k^2} W \sinh s_1 z, \\
g_2 &= -\frac{s_2}{k} W \cosh r_1 z + \frac{s_2}{k} Y \cosh s_1 z \\
&\quad - \frac{k}{r_1} Z \sinh r_1 z + \frac{s_1}{k} X \sinh s_1 z, \\
g_3 &= \frac{r_2}{k} Y \cosh r_1 z - \frac{r_2}{k} W \cosh r_1 z \\
&\quad + \frac{r_1}{k} X \sinh r_1 z - \frac{k}{s_1} Z \sinh s_1 z, \\
g_4 &= Z \cosh r_1 z - X \cosh s_1 z \\
&\quad + \frac{r_1 s_2}{k^2} W \sinh r_1 z - \frac{s_2}{s_1} Y \sinh s_1 z.
\end{aligned} \tag{22}$$

Hence, if $\det G_H \neq 0$ (This is shown in 2.4), (20) is solved for (P', A') in the form

$$\begin{pmatrix} P' \\ A' \end{pmatrix} = \frac{k^2}{k^3} G_H^{-1} \begin{pmatrix} u_H^* \\ w_H^* \end{pmatrix}. \tag{23}$$

Now, (19) holds not only at $z = H$ but also at arbitrary z :

$$G_z \cdot \begin{pmatrix} P' \\ A' \end{pmatrix} = \frac{k^2 \beta_1}{k^3} \begin{pmatrix} u_z^* \\ w_z^* \end{pmatrix}. \tag{24}$$

Therefore, substituting (23) into (24), we obtain

$$\begin{pmatrix} u_z^* \\ w_z^* \end{pmatrix} = G_z \cdot G_H^{-1} \cdot \begin{pmatrix} u_H^* \\ w_H^* \end{pmatrix}. \tag{25}$$

Consequently, when $\det G_H^{-1}$ is not equal to 0, the mapping F from (u_H^*, w_H^*) to (u_z^*, w_z^*) is obtained as

$$F = G_z \cdot G_H^{-1}, \tag{26}$$

where G_z is given in (21),(22).

2.3 Example; Application of the mapping F to a sinusoidal boundary condition

Let us consider tactile exploration at the constant velocity v_0 . As a basic fourier component of the displacement of the finger surface at that time, we take a sinusoidal z -directional displacement with the spatio-temporal frequency (k_0, ω_0) , where $\omega_0 = k_0 v_0$. That is to say, the inverse image of F is given as

$$\begin{aligned}
\begin{pmatrix} u_H \\ w_H \end{pmatrix} &= \begin{pmatrix} 0 \\ A \cos K(x + v_0 t) \end{pmatrix} \\
\iff \begin{pmatrix} u_H^* \\ w_H^* \end{pmatrix} &= \begin{pmatrix} 0 \\ A \delta(k - k_0, \omega - k_0 v_0) \end{pmatrix}.
\end{aligned} \tag{27}$$

Then, applying the mapping F in (26) to (27), we can obtain the basic amplitude distribution inside the finger in tactile exploration.(Fig.3)

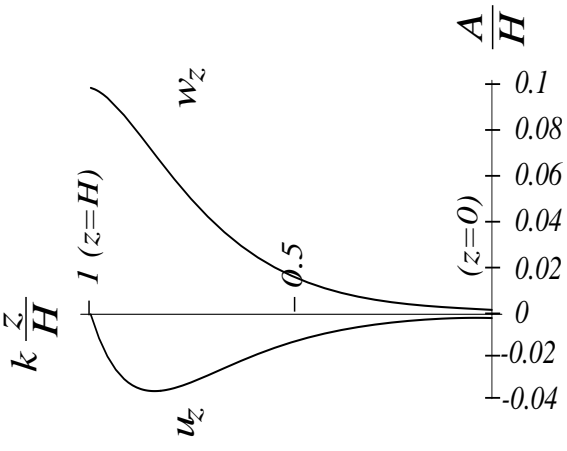


Figure 3: **Amplitude distribution inside the finger in exploring a sinusoidal shape.** ($A=0.1$ [mm], $H=1$ [mm], $\lambda_0 = \frac{2\pi}{k_0}=1$ [mm])

2.4 The mapping F is one-to-one

Let us consider the boundary condition of a traveling wave with velocity v_0 , where $v_0 < \alpha_i, \beta_i$. Then, the mapping F in (26) holds for the next theorem.

Theorem If $\mu = \frac{\mu_2}{\mu_1} < 1$ in the two-layered elastic half space, F is a one-to-one mapping.

This theorem shows that the displacement inside a two-layered elastic medium is uniquely determined by the displacement of the surface if $\mu < 1$, that is, the upper layer is stiffer than the lower layer. According to [11], the human finger has

$$\mu_1 = 6 \times 10^5 [\text{Pa}], \quad \mu_2 = 2 \times 10^5 [\text{Pa}], \quad \text{hence } \mu = \frac{1}{3} < 1.$$

Thus, the finger satisfies the assumption of the theorem, and the mapping from the displacements of the skin surface to the displacements of the mechanoreceptor is one-to-one. Therefore, it is necessary to reproduce the real finger surface displacements in order to generate the same mechanoreceptors displacements as in real tactile exploration.

In the proof of this theorem (Appendix), the condition, $\mu < 1$, is essential. When $\mu > 1$, the example that F is many-to-one can be constructed[15]. It should be noted that human skin has $\mu < 1$ structure which does not lose the quality of tactile information.

3 The principle of Many-to-one VR

According to the theorem above, the displacement of the finger surface should be identical with the displacement in real exploration for tactile VR. Then, before the mapping F , the mapping C from shapes of objects to displacements of the finger surface is considered next. C is determined by physics of contact between the skin and the object. So in this section, we discuss the many-to-one property of C , and investigate a possibility to form the same displacement of the finger surface as in real exploration without generating the real shape of the object. (Fig. 1)

3.1 Amplitude modulated, almost sinusoidal traveling wave

Let us consider the superposition of traveling waves with spatio-temporal frequencies (k_1, ω_1) and (k_2, ω_2) . The shape of this wave is

$$\begin{aligned} & \cos(\omega_1 t - k_1 x) + \cos(\omega_2 t - k_2 x) \\ = & 2 \cos\left(\frac{\omega_1 - \omega_2}{2} t - \frac{k_1 - k_2}{2} x\right) \cos\left(\frac{\omega_1 + \omega_2}{2} t + \frac{k_1 + k_2}{2} x\right). \end{aligned} \quad (28)$$

The first factor of (28) represents the envelope wave of the amplitude-modulated, almost sinusoidal traveling wave whose

- spatial frequency is $k_{mod} = \frac{k_1 - k_2}{2}$,
 - temporal frequency is $\omega_{mod} = \frac{\omega_1 - \omega_2}{2}$,
 - modulated velocity is $v_g = \frac{\omega_{mod}}{k_{mod}} = \frac{\omega_1 - \omega_2}{k_1 - k_2}$.
- (29)
- $\gamma = 10^3$ (when the frequency is 100[Hz]) $\sim 5 \times 10^3$ (when 1[kHz]) [dyne sec/cm²]
 - $m = 1$ [g/cm³]
 - $\frac{k}{m} = 2\pi \times 30 \sim 2\pi \times 40$ [1/s].

Now we consider touching the amplitude modulated traveling wave with the finger. If the skin detects the envelope of the wave, an arbitrary displacement on the finger surface can be produced because the frequencies (k_{mod}, ω_{mod}) is arbitrarily controllable by $(k_1, \omega_1), (k_2, \omega_2)$ as shown in (29). The advantage of this method is unnecessary to prepare all the objects with arbitrary shapes.

The following two points must be confirmed for this method.

- The skin detects the envelope of the amplitude-modulated traveling wave. In other words, C has the many-to-one property. \rightarrow Discussed in 3.2.
- Amplitude modulated waves whose frequencies (k_{mod}, ω_{mod}) are controllable can indeed be formed in some medium. \rightarrow Discussed in 3.3.

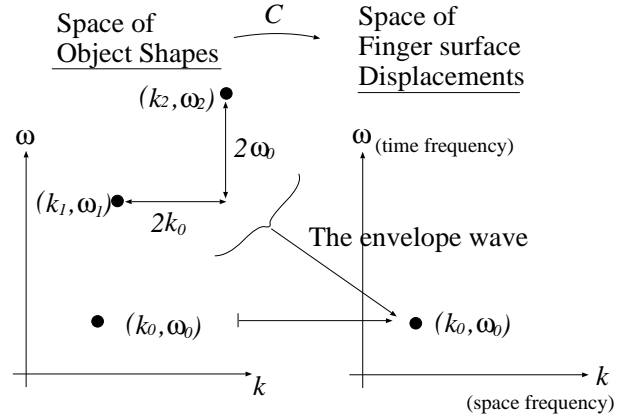


Figure 4: The many-to-one property of C

3.2 The non-linearity of the skin

Let us consider the skin model composed of a spring (k), a mass (m), and a damper (γ). The essence of the contact is a one-directional transmission of the force; that is, the object can only push the skin inside. Thus, the movement of the skin is the damped oscillation when the vibrating object is removed from the skin. Therefore, the skin detects the envelope of the displacement of the object vibrating with an adequately high frequency. Indeed, according to [7],

$$\Rightarrow \frac{-\gamma + \sqrt{\gamma^2 - 4mk}}{2m} \simeq 50[1/s] \sim 10[\text{Hz}].$$

Hence, the skin can detect the vibration with a frequency of more than 10[Hz].

3.3 The method to form amplitude-modulated traveling waves – using the elastic wave called 'Lamb wave'

We use Lamb waves to form amplitude-modulated traveling waves. The Lamb wave is a traveling wave in an infinite elastic plate. There exists infinite symmetric(longitudinal) and anti-symmetric(flexural) modes, whose dispersion curves are shown in Fig.5.

To form the envelope wave with modulated velocity is v_0 , a line is drawn with the gradient $v_0 = \frac{\omega_0}{k_0}$ on the frequency plane. Let $(k_1, \omega_1), (k_2, \omega_2)$ be the frequencies determined by the intersecting points of the line

and the dispersion curves. Then the superposition of the two Lamb waves with frequencies $(k_1, \omega_1), (k_2, \omega_2)$ provides the envelope wave with modulated velocity v_0 .

Especially for $v_0 = 0$, the immovable envelope is obtained by the two Lamb waves which have the same temporal frequencies.

An arbitrary wave number k_0 is obtained by the parallel movement of the line. For small k_0 , we choose the intersecting points on the dispersion curves of two modes which approach the same asymptote at high frequency. For large k_0 , the first and the higher modes are used.

From the above discussions, we obtain the principle of the tactile display using elastic waves as follows:

The principle of the tactile display

To provide tactile sensations of exploring an object with the spatial frequency k_0 at the velocity v_0 , we superpose two Lamb waves whose envelope wave has the spatial frequency k_0 , and the modulated velocity v_0 . This condition is fulfilled by generating two Lamb waves with spatio-temporal frequencies $(k_1, \omega_1), (k_2, \omega_2)$ which satisfy

$$k_1 - k_2 = 2k_0, \quad \omega_1 - \omega_2 = 2\omega_0.$$

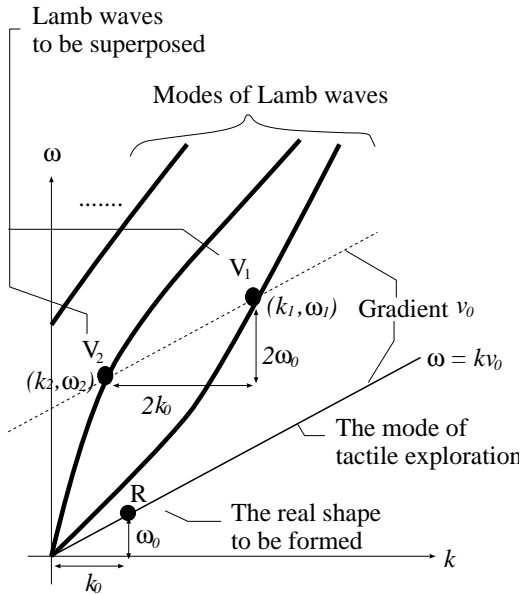


Figure 5: **The method to display the sensation in tactile exploration by amplitude-modulated Lamb waves.** The same displacements of the finger surface are created by using either R or $V_1 + V_2$.

4 Experiments

4.1 Construction

Studies on the ultrasonic linear motor using elastic traveling waves provide clues to forming Lamb waves on the elastic plate.[14] Although the Lamb wave with a single frequency is vibrated on the metal plate (or stick) in the motor, many Lamb waves of different modes should be vibrated at the same time in the tactile display. Here, the first symmetric and the first anti-symmetric Lamb wave are used. The construction of the display is as follows:

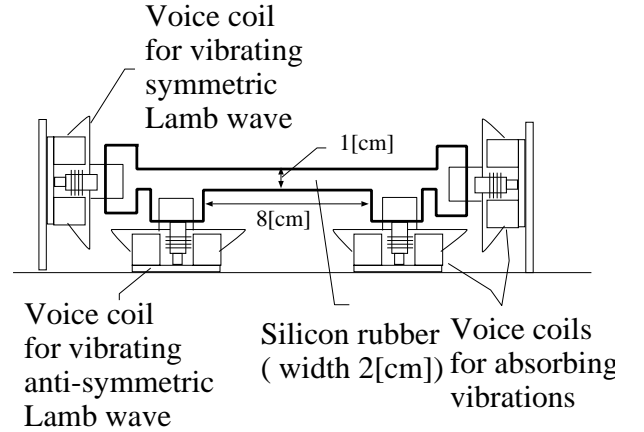


Figure 6: **The construction of the tactile display.**

The voice coil perpendicular to the plate vibrates the first anti-symmetric Lamb wave (flexural wave), and the voice coil parallel to the plate vibrates the first symmetric Lamb wave (longitudinal wave). We vibrate the plate by the voice coil on one side of the plate, and absorb the vibration by the coil on the other side. When an impedance of the voice coil for absorbing vibrations is matched to an impedance of the plate, the traveling wave is created. Thus, the traveling wave toward any direction can be generated by changing the role of the voice coils in both sides. We use $8[\Omega], 50[W]$ woofers as voice coils.

4.2 Material

The main aim of the experimental device here is to confirm the generation of an amplitude-modulated Lamb wave. We use the low temporal frequency so as to obtain a large amplitude. However, the spatial frequency of the Lamb wave decreases with a lowering of the frequency of the vibration, which results in the decrease of spatial resolution of the tactile display. Thus, we use silicon rubber, which has a low Young's ratio, to keep the temporal frequency low, and the spatial

frequency high. The dispersion curves of this silicon rubber shows the possibility of creating a Lamb wave with the wave length in the order of a few centimeters, by the audio frequency.

4.3 Result

By vibrating longitudinal and flexural modes with 30[Hz] at the same time, we can obtain the amplitude-modulated Lamb wave, which is shown in Fig. 7. The phenomenon that the envelope wave progresses, that is, the modulated velocity is not equal to zero, is also confirmed.

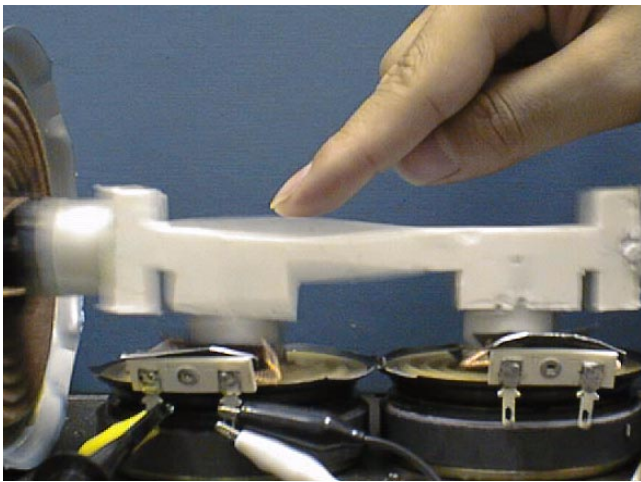


Figure 7: **Experiment— touching the envelope of the amplitude-modulated Lamb wave.** The curve touched by the finger is the envelope wave. By controlling two frequencies of the voice coils, we can generate an envelope wave with an arbitrary wave length and modulated velocity.

4.4 Future work

The amplitude-modulated Lamb wave whose modulated velocity is controllable can be generated in our display. Now the frequencies are held at 30[Hz] to obtain a large amplitude, but next, we vibrate the plate at higher frequencies in order that human does not feel the vibration of the carrier wave. Higher temporal frequencies also provide higher spatial frequencies, which result in the higher spatial resolution.

To produce traveling waves at high frequencies, it is necessary to match the impedance of the voice coils and the plate more precisely.

5 Conclusion

In this paper, the phenomena inside a human finger in tactile exploration have been analyzed with a

two-layered, elastic half space model of the finger. We derived the expression of the mapping from the displacement of the finger surface to the displacement of the mechanoreceptors, and showed that it is one-to-one owing to its characteristic structure — the upper layer of the finger being stiffer than the lower. Next, the mapping from the object shape to the displacement of the finger surface was considered, and shown to be many-to-one because of the mechanical character of the skin. Then we proposed the tactile display using the many-to-one property as follows: The amplitude-modulated traveling wave by the superposition of the first longitudinal and the first flexural Lamb wave on the elastic plate produces its envelope shape on the finger surface, whose spatial frequency and moving velocity can be arbitrarily controlled. With the experimental device of silicon rubber vibrated by voice coils, we have confirmed the generation of an envelope wave. To control the wave number of the envelope wave arbitrarily, the additional study on vibrating the traveling wave of a single mode to a large degree of certainty is necessary.

References

- [1] R.D.Howe, et al., "Remote palpation Technology," *IEEE engineering in Medicine and Biology*, Vol.14, No.3, pp. 318-323.
- [2] Y.Ikei, K.Wakamatsu, S.Fukuda, "Texture presentation by vibratory tactile display," *Proc. VRAIS '96*, IEEE, pp. 199-205.
- [3] M.Shimojo, M.Shinohara, Y.Fukui, "Shape identification performance and pin-matrix density in a 3 dimensional tactile display," *Proc. VRAIS '96*, IEEE, pp. 180-187.
- [4] G.C.Burdea, *Force and touch feedback for virtual reality*, Wiley interscience, 1994.
- [5] J.R.Phillips, K.O.Johnson, "Tactile Spatial Resolution-III. A Continuum Mechanics Model of Skin Predicting Mechanoreceptor Responses to Bars, Edges, and Gratings," *J.Neurophysiol.*, Vol. 46, No. 6, pp. 1204-1225, 1981.
- [6] Srinivasan M.A. and Dandekar K, "An investigation of the mechanics of tactile sense using two dimensional models of the primate fingertip," *Journal of Biomechanical Engineering*, Vol 118, pp. 48-55, 1996.
- [7] H.E.Gierke et al., "Physics of Vibrations in Living Tissues," *Journal of applied Physiology*, 4, 886-900, 1951.

- [8] T.J.Moore, "A Survey of the Mechanical Characteristics of Skin and Tissue in Response to Vibratory Stimulation," *IEEE Transactions on Man-Machine Systems*, Vol. 11, No.1, pp. 79-84, 1970.
- [9] R.O.Potts et al., "The Dynamic Mechanical Properties of Human Skin *in vivo*," *Journal of Biomechanics*, Vol. 16, No. 6, pp. 365-372, 1983.
- [10] H.E.Pereira, "Analysis of Shear Wave Propagation in Skin," *Journal of Biomechanics*, Vol. 23, pp. 745-751, 1990.
- [11] H.E.Pereira et al., "The Effects of Layer Properties on Shear Disturbance Propagation in Skin," *Transactions of the ASME*, Vol. 113, pp. 30-35, 1991.
- [12] W.M.Ewing, *Elastic Waves in Layered Media*, Frank press, 1957
- [13] A.E.H.Love, *Some problems of Geodynamics*, Dover publications, 1911
- [14] M.Kuribayashi, S.Uehara, E.Mori, "Excitation conditions of flexural traveling waves for a reversible ultrasonic linear motor," *Journal of the Acoustical Society of America*, 77(4), April, 1985
- [15] T.NARA, "Tactile Display using Elastic Waves," *University of Tokyo Master Thesis*, 1997 (in Japanese)

Appendix – Proof of the theorem in 2.4

First, we represent $\det G_z$ as a function of z . The expression is obtained from (21),(22) as

$$\begin{aligned}
\det G_z &= g_1 \cdot g_4 - g_2 \cdot g_3 \\
&= 2 \left(-XZ + \frac{r_2 s_2}{k^2} YW \right) \\
&+ \frac{1}{2} \cosh(r_1 + s_1) z \cdot \left[\left(1 - \frac{r_1 s_1}{k^2} \right) \left(X^2 - \frac{r_2 s_2}{k^2} W^2 \right) \right. \\
&\quad \left. + \left(1 - \frac{k^2}{r_1 s_1} \right) \left(Z^2 - \frac{r_2 s_2}{k^2} Y^2 \right) \right] \\
&+ \frac{1}{2} \cosh(r_1 - s_1) z \cdot \left[\left(1 + \frac{r_1 s_1}{k^2} \right) \left(X^2 - \frac{r_2 s_2}{k^2} W^2 \right) \right. \\
&\quad \left. + \left(1 + \frac{k^2}{r_1 s_1} \right) \left(Z^2 - \frac{r_2 s_2}{k^2} Y^2 \right) \right] \\
&+ \frac{1}{2} \sinh(r_1 + s_1) z \cdot \left(\frac{r_2}{r_1} + \frac{s_2}{s_1} \right) \left(1 - \frac{r_1 s_1}{k^2} \right) (XY - ZW) \\
&+ \frac{1}{2} \sinh(r_1 - s_1) z \cdot \left(\frac{r_2}{r_1} - \frac{s_2}{s_1} \right) \left(1 + \frac{r_1 s_1}{k^2} \right) (XY - ZW).
\end{aligned}$$

A necessary and sufficient condition of F being one-to-one is $\det G_z \neq 0$. To prove $\det G_z \neq 0$, we show

- i) $\det G_{z=0} > 0$,
ii) $\det G$ is a monotone increasing function of z ,

as follows:

$$\begin{aligned}
\text{i) } \det G_{z=0} &= \left(1 - \sqrt{1 - \frac{v^2}{\alpha_2^2}} \sqrt{1 - \frac{v^2}{\beta_2^2}} \right) \frac{k_{\beta_1}^4}{k^4} > 0 \\
&\quad \text{(because of the assumption; } v < \alpha_i, \beta_i) \\
\text{ii) } \frac{d}{dz} \det G_z &= \frac{1}{2} (r_1 + s_1) \sinh(r_1 + s_1) z \\
&\cdot \left[\left(1 - \frac{r_1 s_1}{k^2} \right) \left(X^2 - \frac{r_2 s_2}{k^2} W^2 \right) + \left(1 - \frac{k^2}{r_1 s_1} \right) \left(Z^2 - \frac{r_2 s_2}{k^2} Y^2 \right) \right] \\
&+ \frac{1}{2} (r_1 - s_1) \sinh(r_1 - s_1) z \\
&\cdot \left[\left(1 + \frac{r_1 s_1}{k^2} \right) \left(X^2 - \frac{r_2 s_2}{k^2} W^2 \right) + \left(1 + \frac{k^2}{r_1 s_1} \right) \left(Z^2 - \frac{r_2 s_2}{k^2} Y^2 \right) \right] \\
&+ \frac{1}{2} (r_1 + s_1) \cosh(r_1 + s_1) z \cdot \left(\frac{r_2}{r_1} + \frac{s_2}{s_1} \right) \left(1 - \frac{r_1 s_1}{k^2} \right) (XY - ZW) \\
&+ \frac{1}{2} (r_1 - s_1) \cosh(r_1 - s_1) z \cdot \left(\frac{r_2}{r_1} - \frac{s_2}{s_1} \right) \left(1 + \frac{r_1 s_1}{k^2} \right) (XY - ZW). \tag{30}
\end{aligned}$$

Here, from the assumption; $\alpha_1 > \beta_1 > v$,

$$r_1 - s_1 = k \left(\sqrt{1 - \frac{v^2}{\alpha_1^2}} - \sqrt{1 - \frac{v^2}{\beta_1^2}} \right) > 0.$$

Therefore, $\frac{d}{dz} \det G_z > 0$, if the coefficients of the four terms in (30) are positive. As for the second term in (30), for example,

$$\begin{aligned}
\cdot X^2 - \frac{r_2 s_2}{k^2} W^2 &> \left(1 - \frac{r_2 s_2}{k^2} \right) W^2 \\
&= \left(1 - \sqrt{1 - \frac{v^2}{\alpha_2^2}} \sqrt{1 - \frac{v^2}{\beta_2^2}} \right) W^2 > 0, \\
\cdot Z^2 - \frac{r_2 s_2}{k^2} Y^2 &> \left(1 - \frac{r_2 s_2}{k^2} \right) Y^2 \\
&= \left(1 - \sqrt{1 - \frac{v^2}{\alpha_2^2}} \sqrt{1 - \frac{v^2}{\beta_2^2}} \right) Y^2 > 0,
\end{aligned}$$

because $\mu < 1 \implies |X| > |W|, |Z| > |Y|$. The other three coefficients are shown to be positive in the same way. (Q.E.D)